

**Different pathways to anomalous stabilization of ice layers on methane hydrates**Y. Li <sup>1,2,\*</sup>, I. Brevik <sup>3</sup>, O. I. Malyi <sup>4</sup>, and M. Boström <sup>4,†</sup><sup>1</sup>*School of Physics and Materials Science, Nanchang University, Nanchang 330031, China*<sup>2</sup>*Institute of Space Science and Technology, Nanchang University, Nanchang 330031, China*<sup>3</sup>*Department of Energy and Process Engineering, Norwegian University of Science and Technology, NO-7491 Trondheim, Norway*<sup>4</sup>*Centre of Excellence ENSEMBLE3 Sp. z o. o., Wolczynska Strasse 133, 01-919, Warsaw, Poland*

(Received 6 March 2023; accepted 3 August 2023; published 5 September 2023)

We explore the Casimir-Lifshitz free-energy theory for surface freezing of methane gas hydrates near the freezing point of water. The theory enables us to explore different pathways, resulting in anomalous (stabilizing) ice layers on methane hydrate surfaces via energy minimization. Notably, we will contrast the gas hydrate material properties, under which thin ice films can form in water vapor, with those previously predicted to be required in the presence of liquid water. It is predicted that methane hydrates in water vapor near the freezing point of water nucleate ice films, instead of water films.

DOI: [10.1103/PhysRevE.108.034801](https://doi.org/10.1103/PhysRevE.108.034801)**I. INTRODUCTION**

The work of Elbaum and Schick [1] on the Casimir-Lifshitz (CL) interaction in ice-water systems has piqued the interest of scientists [2–7]. As we will demonstrate, an extension sheds light on the formation of ice layers on gas hydrates, which are found in ice-cold water [8], the ocean seabed [9], sediments [10], and in permafrost [11]. Gas hydrates can exist as crystalline structures comprising water molecules arranged in cages that enclathrate guest gas molecules [12]. As is well understood, the gas molecules are essential for thermodynamic stability of the structure [12], and bulk clathrates only exist above a certain occupancy of gas molecules. These structures are furthermore stable only within a limited range of temperatures and pressures. However, it was predicted that a surface region of lower occupancy can exist being stabilized by intermolecular forces [13–15]. With reliable, experimentally derived dielectric properties of ice and water [16], Boström *et al.* initiated the theoretical work that predicted relatively thick ice layers on partially degassed hydrates, demonstrating a previously unconsidered mechanism for the stabilization of gas hydrates in cold water [14]. In light of our past work on the anomalous stability of gas hydrates in a liquid water environment [13–15], we demonstrate an alternative pathway for how ice can form at a methane hydrate surface in the presence of cold water vapor (i.e., in the absence of liquid water). Notably, experiments have indeed shown that such ice layers can form in a vapor environment [17]. Second, we contrast the surface properties of the gas hydrate required to achieve anomalous stability in the presence of water vapor, compared to the previously studied cases of gas hydrates in liquid water.

As an experimentally well-known effect [12,17–21], termed “self-preservation,” it was previously assumed that ice layers were created through kinetics, causing gas molecules to deplete in the gas hydrate surface region and the surface molecular structure to reconstruct into an ice-like one. Our previous works, as well as the observation of stable shallow hydrates [22–24], suggested that, under favorable conditions, the formation of the ice layer on the hydrate is not driven purely by kinetics, but also by influences on thermal equilibrium from the CL interaction. Surface tension effects can, to some extent, be assumed constant in quasiplanar geometry as the ice layer thickness varies, motivating that the CL stress can contribute nontrivially. Particularly, the formation of ice layers on methane hydrates in the cold water, arising from the CL interaction, was forecasted and estimated to be almost micron-sized, or at least much more than several tens of nanometers. For micron-sized ice layers, the thermal fluctuation has impacts on the growth of ice layers. These findings, along with the well-documented observation of the self-preservation of hydrates, suggest that the CL interaction could play an important role in understanding self-preservation in gas transport technology, geotechnical and global environmental risk assessments, and other relevant contexts. If the ice-coating on hydrates is indeed spontaneous, resulting in lowering Gibbs free energy as we find, it adds weight to the argument that gas hydrates may be stabilized in a mechanism not previously understood, highlighting the necessity to fully understand the role of CL interaction in the formation and self-preservation of hydrates.

In this work, we describe the theory and predict the phenomenon, stemming from the CL interaction, that different external conditions can bring about different pathways to self-preservation. We define a wet pathway as the case in which the outer surface of the gas hydrate is in contact with a bulk water reservoir. In contrast, for the dry pathway, this outer surface is in contact with water vapor. As shown below, some gas hydrates in water gain the ice-coating interface, whereas others

\*leon@ncu.edu.cn

†mathias.bostrom@ensemble3.eu

have a wet surface. The surface properties of gas hydrates, required to achieve ice layer formation in water, deviate from those in cold water vapor. We revisit the *wet pathway*, through which ice layers form on hydrates immersed in a bulk of ice-cold water, and propose an alternative *dry pathway*, where ice layers form between hydrates and the water vapor. The dry pathway leads to thick ice layers, specifically a layered methane hydrate-ice-water-vapor configuration. The dry pathway is investigated with an alternative inhomogeneous CL theory [25–28]. The water layer in the dry pathway appears at the ice-vapor interface via the structural force [29]. The required surface properties to establish an anomalous ice layer follow from the classical arguments on Casimir-Lifshitz free energy, where the intermediate layer grows when it has dielectric properties in between the surrounding media [30]. Therefore, ice formation through the wet pathway requires a partly gas-depleted surface region, while the dry pathway, in contrast, needs a sufficiently high gas occupancy in the surface region of the gas hydrate.

## II. THEORY AND BACKGROUND

We address the Casimir-Lifshitz free energy at finite temperature by utilizing recently reported dielectric functions for ice and water obtained by Luengo-Márquez and MacDowell [27]. The quadruple point of methane hydrate (MH), very close to the triple point of water, is at about  $T = 272.9$  K,  $p = 25.63$  bar [31]. All materials involved are considered to be near or at this temperature. As in Refs. [13,14], we model the dielectric function of MH ( $\epsilon_{mh}$ ) using a Lorentz-Lorenz model [32] with the mixing scheme for each gas hydrates from Bonnefoy *et al.* [33,34],

$$\epsilon_{mh} = \frac{1 + 2\Gamma}{1 - \Gamma}, \quad \Gamma = \frac{\epsilon_3 - 1}{\epsilon_3 + 2} \left( \frac{n_{wh}}{n_i} \right) + \frac{4\pi\alpha_M n_M}{3}. \quad (1)$$

As reported earlier, quantum chemical calculations of dynamic polarizabilities at discrete frequencies can be represented at arbitrary imaginary frequencies  $i\xi$  by fitting to an oscillator model

$$\alpha_M(i\xi) = \sum_j \frac{\alpha_j}{1 + (\xi/\omega_j)^2}. \quad (2)$$

A five-mode fit as performed by Parsons has been found to describe the dynamic polarisability accurately to a 0.02% relative error [35]. The adjusted parameters for a five-mode model were given in the work by Fiedler *et al.* [36]. The important factors for the dielectric function of MH include the effective ice permittivity weighted by the density of water molecules in hydrates relative to pure ice, and the polarizability of methane molecules [36] and weighted with the gas density. The mass density of water in pure ice is  $0.9167$  g/cm<sup>3</sup> [37], giving the number density of water molecules in pure ice as  $n_i = 3.064 \times 10^{-2}$  Å<sup>-3</sup>. The gas hydrate corresponds to water molecules and gas molecules in a specific structure. Here we consider the full range of gas molecule occupancies, from fully occupied to zero occupancy. The number densities of gas molecules ( $n_M$ ) and water molecules ( $n_{wh}$ ) in different gas hydrate structures are derived using the gas-water number density relation:  $n_M = (N_g \times n_{wh})/46$ , where  $n_{wh} = 2.657 \times 10^{-2}$  Å<sup>-3</sup> and  $N_g = 0-8$  is the number of gas

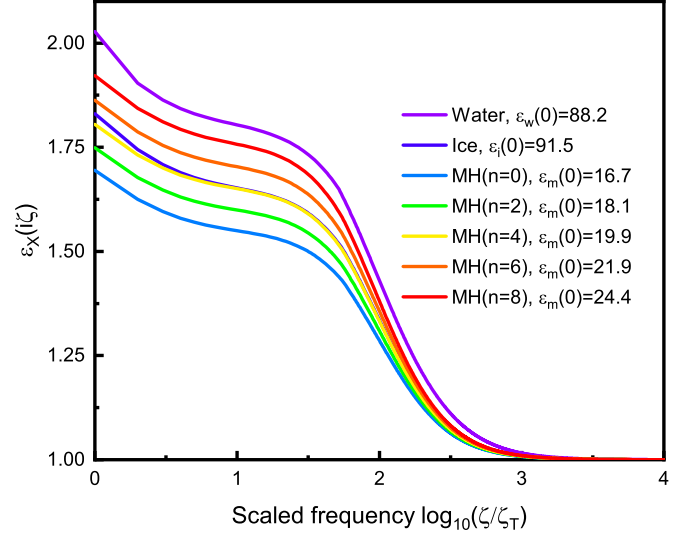


FIG. 1. The dependence of dielectric functions  $\epsilon_X(i\xi)$  on the imaginary frequency  $\xi$ , with the subscript X signifying the materials water, ice, and MH.  $n$  is the occupancy number of the MH. The corresponding static values of dielectric functions are listed.

molecules per 46 water molecules in the structure. The gas hydrate number densities were derived following the work by Prieto-Ballesteros *et al.* [38] (and references therein). As the occupancy of the gas hydrate changes, that is, gas molecules are absorbed into or separated from the hydrate, the dielectric properties of the gas hydrate change accordingly, resulting in totally different behaviors as we shall see in the following sections. Those dielectric functions involved in this work are schematically demonstrated in Fig. 1.

We consider MHs covered with an ice layer that is sufficiently wide to be treated as locally planar. A schematic illustration of our model system is shown in Fig. 2. It dates back to 1950 and 1960s, when the Casimir-Lifshitz interaction in the layered planar dielectric system was considered by Landau *et al.* [30,39] in terms of the macroscopic Maxwell equations with the fluctuating polarization. The approach based on the Green's function is now more widely employed. For multilayer systems, some of the authors followed this approach and evaluated the CL interaction there with the theory of inhomogeneous CL interactions [40]. (For more details, please refer to the Appendix of Ref. [15].) The CL free energy per unit area at temperature  $T$ , for a five-layer configuration as an instance, is obtained as in Refs. [15,26,41]

$$F_{CL}(d) = \frac{T}{2\pi} \sum_{m=0}^{\infty} \int_0^{\infty} dk k \sum_{s=E,H} \ln \left[ 1 + r_{12}^s r_{23}^s e^{-2\kappa_2 d_2} + r_{23}^s r_{34}^s e^{-2\kappa_3 d_3} + r_{34}^s r_{45}^s e^{-2\kappa_4 d_4} + r_{12}^s r_{34}^s e^{-2(\kappa_2 d_2 + \kappa_3 d_3)} + r_{23}^s r_{45}^s e^{-2(\kappa_3 d_3 + \kappa_4 d_4)} + r_{12}^s r_{23}^s r_{34}^s r_{45}^s e^{-2(\kappa_2 d_2 + \kappa_4 d_4)} + r_{12}^s r_{45}^s e^{-2(\kappa_2 d_2 + \kappa_3 d_3 + \kappa_4 d_4)} \right], \quad (3)$$

where  $k$  is the modulus of the wave vector  $\mathbf{k}$  parallel to the surface,  $\kappa_i = \sqrt{k^2 + \epsilon_i \xi_m^2}$  with  $i = 1, \dots, 5$  labeling layers in the five-layer system with the layer-stacking order 1–2–3–4–5,  $\xi_m = 2\pi mT$  being the  $m$ th Matsubara frequency,

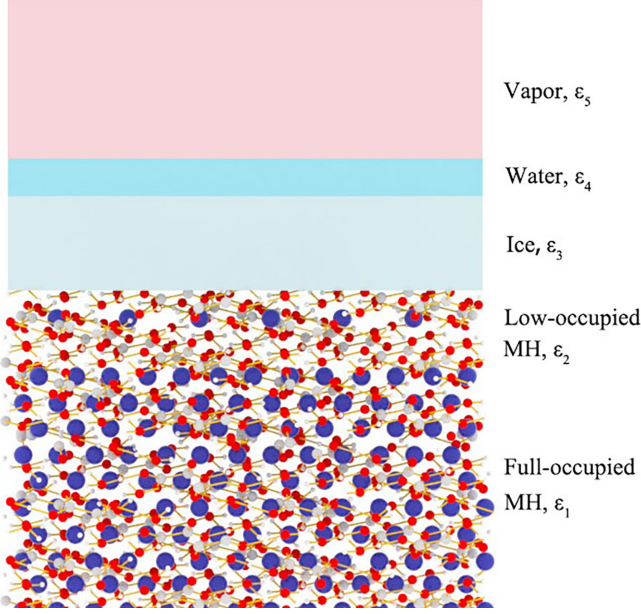


FIG. 2. Schematic diagram of the five-layer system  $\text{CH}_4$  hydrate system: high-occupancy (HO) gas hydrate  $\epsilon_1$ ; low-occupancy (LO) hydrate,  $\epsilon_2$ ; pure  $\text{H}_2\text{O}$  ice,  $\epsilon_3$ ; pure liquid  $\text{H}_2\text{O}$ ,  $\epsilon_4$ , and vapor,  $\epsilon_5$ . In the wet pathway, the water layer is assumed to first go to infinite thickness (i.e., we consider a bulk water reservoir). In the dry pathway, the outer surface is in contact with water vapor.

and  $d_i$ ,  $i = 2, 3, 4$  being the thickness of the  $i$ th layer in this configuration. The primed sum means the zeroth term ( $m = 0$ ) is weighted in half. (The natural unit  $\hbar = c = \epsilon_0 = \mu_0 = k_B = 1$  is employed, unless specified otherwise.) The  $s = E$  and  $s = H$  signify the contributions from the transverse electric (TE) and transverse magnetic (TM) modes, respectively. The reflection coefficients at the interface between the  $i$ th and  $j$ th layers are defined as [41]

$$r_{ij}^E = \frac{\kappa_i - \kappa_j}{\kappa_i + \kappa_j}, \quad r_{ij}^H = \frac{\epsilon_j \kappa_i - \epsilon_i \kappa_j}{\epsilon_j \kappa_i + \epsilon_i \kappa_j}. \quad (4)$$

The CL free energy for the four- and three-layer systems can be obtained with Eq. (3), by setting the materials of properly chosen adjacent layers the same [15,26,27]. When accounting for structural forces related to the packing of water molecules on the solid ice substrate [29,42], an atomically thin water layer arises on the interface between the anomalous-stabilizing ice layer and the vapor, which has no effect on the anomalous stabilization in this research, i.e., on how effective the ice layer prevents the leakage of methane molecules.

### III. RESULTS AND DISCUSSIONS

In this work, we focus on pathways for the anomalous stabilization of ice layers on MHs with various occupancies of gas molecules and in different environments, and mostly investigate corresponding three-layer configurations. Brief discussions on the minor four-layer contributions are given. Although we have relatively simple formulas for the CL free energy, a practically analyzable expression for such of a system here, consisting of real materials, is still beyond reach. In this paper, we mainly resort to numerical evaluations,

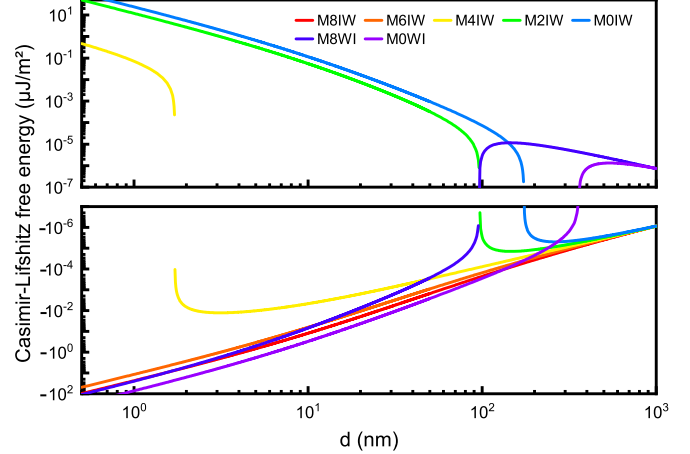


FIG. 3. The Casimir-Lifshitz free energy per unit area for three-layer configurations MH ( $n_b = i$ )-ice-water (MiIW) and MH ( $n_b = i$ )-water-ice (MiWI) with  $n_b$  being the occupancy number.

based on the dielectric data as mentioned at the beginning of Sec. II.

#### A. Wet pathway for anomalous-stabilizing ice layers

For the bulk MH immersed in the reservoir of ice-cold water, as in Refs. [13,14], the growth of the ice layer, due to the CL interaction, are seen. According to Fig. 3, with a low occupancy ( $n_b < 5$ ), the ice layer forms via a wet pathway and can have a thickness ranging from several to hundreds of nanometers, as this minimizes the CL free energy. The equilibrium ice layer thicknesses for three-layer MH ( $n_b = i$ )-ice-water system for different  $n_b = i$  are given in Table I. In this table we also present the nonretarded Hamaker constants  $A$  and their contributions from the zero frequency terms  $A_0$ , obtained with

$$A = -6T \sum_{m=0}^{\infty} \int_0^{\infty} dk k \ln \left[ 1 - \frac{\epsilon_1 - \epsilon_2}{\epsilon_1 + \epsilon_2} \frac{\epsilon_3 - \epsilon_2}{\epsilon_3 + \epsilon_2} e^{-2k} \right]. \quad (5)$$

TABLE I. The Hamaker constants at  $T = 272.9$  K,  $p = 25.63$  bar [31], using Eq. (5) for  $A$  and its contributions from the zeroth Matsubara term  $A_0$  for various three-layer configurations with methane gas hydrate ( $n_b$ )-ice-water. For each combination with an equilibrium thickness  $d_{\text{eq}}$  (the case with no equilibrium film is marked with -).

$n_b$	$A$ (meV)	$A_0$ (meV)	$d_{\text{eq}}$ (nm)
0	$-6.00 \times 10^0$	$2.25 \times 10^{-1}$	262
1	$-4.51 \times 10^0$	$2.21 \times 10^{-1}$	207
2	$-3.02 \times 10^0$	$2.17 \times 10^{-1}$	146
3	$-1.53 \times 10^0$	$2.13 \times 10^{-1}$	79.3
4	$-3.87 \times 10^{-2}$	$2.09 \times 10^{-1}$	3.13
5	$1.45 \times 10^0$	$2.04 \times 10^{-1}$	-
6	$2.93 \times 10^0$	$2.99 \times 10^{-1}$	-
7	$4.41 \times 10^0$	$1.94 \times 10^{-1}$	-
8	$5.89 \times 10^0$	$2.88 \times 10^{-1}$	-

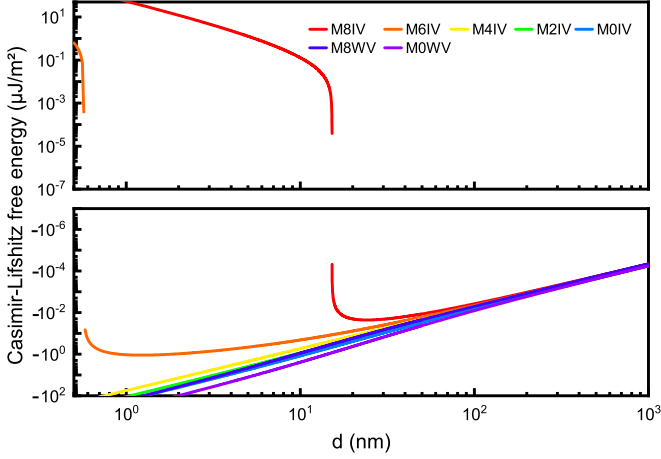


FIG. 4. The Casimir-Lifshitz free energy per unit area for three-layer configurations MH ( $n_b = i$ )-ice-vapor (MiIV) and MH ( $n_b = i$ )-water-vapor (MiWV) with  $n_b$  being the occupancy number.

As is easily seen from Eq. (5), the sign of the three-layer interaction is related to the relative magnitudes [30] of the dielectric functions for the relevant systems (shown in Fig. 1). Notably, systems with short-range repulsion (negative Hamaker constant) and long-range attraction (positive value for zero frequency contribution to Hamaker constant) are the required properties to induce ice layer formation, which is exactly demonstrated by Table I. Therefore, it is foreseeable that when the MH is relatively fully occupied, the three-layer free energy can only be minimized by reducing the thickness of the ice layer to zero, preventing ice formation, or resulting in a wet MH surface. Furthermore, when the MH is in contact with a bulk of ice, instead of water, the CL free energy, thus stressed, prohibits the formation of micron or even nanosized water layers.

### B. Dry pathway for anomalous-stabilizing ice layers

When the MH is exposed to a water vapor environment, the ice layer should exist as demonstrated in Fig. 4, if the MH is quite fully filled ( $n_b > 5$ ), in contrast to the wet path scenario above. That is, this ice layer is formed via the dry pathway. The required properties for the gas hydrate to induce an ice layer via the dry pathway can be understood analogously to how we discussed in the case of the wet pathway. The intermediate layer grows when it has dielectric properties in between the surrounding media [30]. It is clear that this is the case as can be seen in Fig. 1 and from the Hamaker constants presented in Table II. In other words, when ( $n_b > 5$ )  $\varepsilon_{mh} > \varepsilon_i > \varepsilon_v$  for a broad range of finite Matsubara frequencies and  $\varepsilon_i > \varepsilon_{mh} > \varepsilon_v$  for zero frequency, a finite-sized ice layer forms in the dry pathway. In contrast, in the wet pathway ( $n_b < 5$ ) we predict that the condition for a finite-sized ice layer is that  $\varepsilon_w > \varepsilon_i > \varepsilon_{mh}$  for a broad range of finite Matsubara frequencies and  $\varepsilon_i > \varepsilon_w > \varepsilon_{mh}$  for zero frequency. As expected and shown in Fig. 4, a water layer is not present between the MH of any occupancy and the vapor, implying a dry MH surface. Remarkably, if the surface layer is degassed before the anomalous ice coating is formed, the ice cannot form via the dry

TABLE II. The Hamaker constants at  $T = 272.9$  K,  $p = 25.63$  bar [31], using Eq. (5) for  $A$  and its contributions from the zeroth Matsubara term  $A_0$  for various three-layer configurations with methane gas hydrate ( $n_b$ )-ice-vapor. For each combination with an equilibrium thickness  $d_{eq}$  (the case with no equilibrium film is marked with -).

$n_b$	$A$ (meV)	$A_0$ (meV)	$d_{eq}$ (nm)
0	$3.99 \times 10^1$	$1.33 \times 10^1$	-
1	$3.33 \times 10^1$	$1.30 \times 10^1$	-
2	$2.66 \times 10^1$	$1.28 \times 10^1$	-
3	$1.99 \times 10^1$	$1.25 \times 10^1$	-
4	$1.32 \times 10^1$	$1.22 \times 10^1$	-
5	$6.51 \times 10^0$	$1.19 \times 10^1$	-
6	$-1.91 \times 10^{-1}$	$1.16 \times 10^1$	1.22
7	$-6.91 \times 10^0$	$1.12 \times 10^1$	13.8
8	$-1.36 \times 10^1$	$1.09 \times 10^1$	24.1

path, but must rely on the traditional mechanism [12,17–21] via the reorganization of surface layers.

The results above have not yet taken into account the possibility that both ice and water layers can appear on the surface of MH. Furthermore, a bulk of MH usually holds a surface region with lower occupancy, as a result of the rather slow degassing process. Cases like that entail the CL free energy in configurations containing more than three layers, where influences of the thickness of each layer should be examined explicitly. In the four-layer configuration with the media labeled by  $i = 1, 2, 3, 4$  and stacked in the order 1-2-3-4, the CL free energy  $F_{CL}$  can be divided into three parts, namely, the three-layer contributions  $F_{13}$  and  $F_{24}$  from 1-2-3 and 2-3-4, respectively, and the pure four-layer contribution  $F_{14}$ ,

$$F_{tot}(d_2, d_3) = F_{13}(d_2) + F_{24}(d_3) + F_{14}(d_2, d_3), \quad (6)$$

where  $d_i$ ,  $i = 2, 3$  is the thickness of the  $i$ th layer. If the bulk MH in a vapor environment has no degassed surface region, then any four-layer configuration, whether it involves MH-water-ice-vapor or MH-ice-water-vapor, will ultimately converge to the stable state predicted by the corresponding three-layer cases since, in those cases, the additional four-layer contributions are not significant enough to introduce other equilibrium. On the other hand, if a degassed region exists on the surface of bulk MH (the bulk MH is assumed fully filled for simplicity), then the thickness of the surface MH layer can be taken as a constant in the ice-forming process since this surface region changes slowly. The CL free energy counted, therefore, should be the reduced one, obtained by omitting  $F_{13}(d_2)$  in the configuration bulk MH-surface MH- $X$  (water or ice) vapor. The water layer between the surface MH and the vapor is always suppressed as in the three-layer cases in Fig. 3. Similar results apply to the ice layer cases. Moreover, even when the MH material is immersed in cold water or covered by ice, the pure four-layer interaction there, as can be checked, is not enough to significantly modify the stabilities predicted by the three-layer cases.

### C. Discussion on different pathways to self-preservation

It is now widely accepted that anomalous stabilization of ice layers on gas hydrate surfaces can form via kinetics, leading to the reconstruction of the outer layers of the hydrate. However, we demonstrate that ice layers relevant for anomalous stabilization of methane gas hydrates can also form via equilibrium thermodynamics mediated by the Casimir-Lifshitz force. Previous works [14] indicated that a surface region of the gas hydrate with gas molecule depletion was essential. However, this very much depends on the surrounding media. The low occupancy surface required in liquid water is contrasted with a high occupancy surface region essential for ice formation in water vapor. Notably, our theory accounts for two regions (liquid water and ice) growing and receding at each other's expense. Within this theory, Casimir-Lifshitz interactions predict thin dry ice films in water vapor. When structural forces are included [29], together with Casimir-Lifshitz forces, however, we expect an atomically thin liquid water layer. Notably, referring to recent work on ice premelting by MacDowell *et al.* [29], we expect that the outer ice surface can melt via structural forces, leading to a five-layer system with bulk gas hydrate-surface gas hydrate-ice (several tens of nanometers thick)-water (atomically thick)-vapor.

### D. Some theoretical considerations

A comment ought to be given on the fundamental physics of the system analyzed here. Throughout our work, we made use of the continuum electrodynamic theory, even for the small distances between dielectric boundary layers. As is well known, the volume force density in such a layer can be expressed as  $\mathbf{f} = -\frac{1}{2}\epsilon_0 E^2 \nabla \epsilon$  [25,43], and so the surface force density (pressure) is obtained by integrating the normal component  $f_n$  of  $\mathbf{f}$  across the layer. This simple theory works well down to quite low distances of the nanoscale. For even smaller distances, the continuum theory has to be abandoned together with some form of statistical mechanics introduced instead. In this context, note the simulation results recently obtained by Serwatka *et al.* [44] on phase transitions in a one-dimensional chain of water molecules. Since water molecules are rotating, it is possible for the system, at low temperatures (about 10 K), to perform a phase transition to a ferroelectric phase. The physical reason for the increasing interaction between water molecules with decreasing distances is the rise of quantum fluctuations in the ground state. The analyses in Ref. [44] refer primarily to quantum physics. While this area of research is still in its early stages, the results are worth noticing not only from a quantum standpoint, but also from a classical perspective. Behaviors of water molecules at micro or nanoscale distances are complex and extend beyond the scope of the continuum theory.

### IV. WIDER IMPLICATIONS

Clathrates, e.g., methane hydrates, are known to be well-defined crystalline structures with both water molecules and gas molecules. These structures are stable within a limited range of temperatures and pressures. However, methane hydrates were demonstrated to be stable outside their window of stability going to just below the freezing temperature of water [12]. The solution to this unexpectedly wide stability range seems to be that a micron-sized [17] water ice layer forms on the surface [12–14,17]. The formation of an ice layer on the hydrate is not only driven by kinetics, as suggested by Falenty and Kuhs [17], but it can also be driven by Lifshitz-force mediated equilibrium thermodynamics [13,14]. Indeed, since we predict that the self-preserving ice layer effect on hydrates can be spontaneous in both wet and dry systems, this adds additional evidence to the argument that gas hydrates can be stabilized in ways not previously considered.

The important questions are whether the proposed mechanism can be proven experimentally, and whether it has an important environmental impact. Future work should aim to perform measurements on the growth of ice layers on clathrate (e.g., methane hydrate) surfaces in liquid water and in water vapor. We can now state that the energy mechanism does favor ice growth on methane hydrate surfaces under the conditions specified. It is actually likely that there are environmental impacts from such stabilized gas hydrates: Chuvilin, Shakhova *et al.* [22–24] experimentally found that hydrates in permafrost regions appear to exist just below the surface. In addition, hydrates were found outside their expected pressure and temperature stability zones. The current investigation of gas hydrate anomalous preservation is thus both relevant and important in our opinion. Moreover, our study calls for examining additional energy contributions. These include salt [3,45,46], curvature [7], and effects accounting for temperatures [29] below the quadruple point.

### ACKNOWLEDGMENTS

We thank the Terahertz Physics and Devices Group, Nanchang University for the strong computational facility support. The authors thank the “ENSEMBLE3 - Centre of Excellence for nanophotonics, advanced materials, and novel crystal growth-based technologies” project (Grant No. MAB/2020/14) carried out within the International Research Agendas program of the Foundation for Polish Science cofinanced by the European Union under the European Regional Development Fund and the European Union's Horizon 2020 research and innovation program Teaming for Excellence (Grant No. 857543) for the support of this work.

- 
- [1] M. Elbaum and M. Schick, Application of the Theory of Dispersion Forces to the Surface Melting of Ice, *Phys. Rev. Lett.* **66**, 1713 (1991).  
 [2] J. G. Dash, H. Fu, and J. S. Wettlaufer, The premelting of ice and its environmental consequences, *Rep. Prog. Phys.* **58**, 115 (1995).

- [3] J. S. Wettlaufer, Impurity Effects in the Premelting of Ice, *Phys. Rev. Lett.* **82**, 2516 (1999).  
 [4] J. Benet, P. Llombart, E. Sanz, and L. G. MacDowell, Premelting-Induced Smoothing of the Ice-Vapor Interface, *Phys. Rev. Lett.* **117**, 096101 (2016).

- [5] J. Benet, P. Llombart, E. Sanz, and L. G. MacDowell, Structure and fluctuations of the premelted liquid film of ice at the triple point, *Mol. Phys.* **117**, 2846 (2019).
- [6] H. Li, M. Bier, J. Mars, H. Weiss, A. Dippel, O. Gutowski, V. Honkimäki, and M. Mezger, Interfacial premelting of ice in nano composite materials, *Phys. Chem. Chem. Phys.* **21**, 3734 (2019).
- [7] P. Parashar, K. V. Shajesh, K. A. Milton, D. F. Parsons, I. Brevik, and M. Boström, Role of zero point energy in promoting ice formation in a spherical drop of water, *Phys. Rev. Res.* **1**, 033210 (2019).
- [8] G. R. Dickens and M. S. Quinby-Hunt, Methane hydrate stability in seawater, *Geophys. Res. Lett.* **21**, 2115 (1994).
- [9] N. Mahabadi, X. Zheng, and J. Jang, The effect of hydrate saturation on water retention curves in hydrate-bearing sediments, *Geophys. Res. Lett.* **43**, 4279 (2016).
- [10] T.-H. Kwon, G.-C. Cho, and J. C. Santamarina, Gas hydrate dissociation in sediments: Pressure-temperature evolution, *Geochem. Geophys. Geosystems.* **9**, Q03019 (2008).
- [11] *Natural Gas Hydrate in Oceanic and Permafrost Environments*, edited by M. D. Max (Kluwer Academic, Washington, D.C., USA, 2003).
- [12] S. Takeya and J. A. Ripmeester, Dissociation behavior of clathrate hydrates to ice and dependence on guest molecules, *Angew. Chem., Int. Ed.* **47**, 1276 (2008).
- [13] M. Boström, R. W. Corkery, E. R. A. Lima, O. I. Malyi, S. Y. Buhmann, C. Persson, I. Brevik, D. F. Parsons, and J. Fiedler, Dispersion forces stabilize ice coatings at certain gas hydrate interfaces that prevent water wetting, *ACS Earth Space Chem.* **3**, 1014 (2019).
- [14] M. Boström, V. Estesó, J. Fiedler, I. Brevik, S. Y. Buhmann, C. Persson, S. Carretero-Palacios, D. F. Parsons, and R. W. Corkery, Self-preserving ice layers on CO<sub>2</sub> clathrate particles: Implications for Enceladus, Pluto and similar ocean worlds, *Astron. Astrophys.* **650**, A54 (2021).
- [15] Y. Li, R. W. Corkery, S. Carretero-Palacios, K. Berland, V. Estesó, J. Fiedler, K. A. Milton, I. Brevik, and M. Boström, Origin of anomalously stabilizing ice layers on methane gas hydrates near rock surface, *Phys. Chem. Chem. Phys.* **25**, 6636 (2023).
- [16] J. Fiedler, M. Boström, C. Persson, I. H. Brevik, R. W. Corkery, S. Y. Buhmann, and D. F. Parsons, Full-spectrum high resolution modeling of the dielectric function of water, *J. Phys. Chem. B* **124**, 3103 (2020).
- [17] A. Falenty and W. F. Kuhs, “Self-Preservation” of CO<sub>2</sub> Gas Hydrates-Surface Microstructure and Ice Perfection, *J. Phys. Chem. B* **113**, 15975 (2009).
- [18] Y. P. Handa, Calorimetric determinations of the compositions, enthalpies of dissociation, and heat capacities in the range 85 to 270 K for clathrate hydrates of xenon and krypton, *J. Chem. Thermo.* **18**, 891 (1986).
- [19] A. Hallbrucker and E. Mayer, Unexpectedly stable nitrogen, oxygen, carbon monoxide and argon clathrate hydrates from vapour-deposited amorphous solid water: An x-ray and two-step differential scanning calorimetry study, *J. Chem. Soc., Faraday Trans.* **86**, 3785 (1990).
- [20] E. D. Ershov and V. S. Yakushev, Experimental research on gas hydrate decomposition in frozen rocks, *Cold Regions Science and Technology* **20**, 147 (1992).
- [21] A. Hachikubo, S. Takeya, E. Chuvilin, and V. Istomin, Preservation phenomena of methane hydrate in pore spaces, *Phys. Chem. Chem. Phys.* **13**, 17449 (2011).
- [22] N. Shakhova, I. Semiletov, O. Gustafsson, V. Sergienko, L. Lobkovsky, O. Dudarev, V. Tumskoy, M. Grigoriev, A. Mazurov, A. Salyuk, R. Ananiev, A. Koshurnikov, D. Kosmach, A. Charkin, N. Dmitrevsky, V. Karnaukh, A. Gunar, A. Meluzov, and D. Chernykh, Current rates and mechanisms of subsea permafrost degradation in the east Siberian arctic shelf, *Nat. Commun.* **8**, 15872 (2017).
- [23] E. Chuvilin, B. Bukhanov, D. Davletshina, S. Grebenkin, and V. Istomin, Dissociation and self-preservation of gas hydrates in permafrost, *Geosciences* **8**, 431 (2018).
- [24] N. Shakhova, I. Semiletov, and E. Chuvilin, Understanding the permafrost-hydrate system and associated methane releases in the east Siberian arctic shelf, *Geosciences* **9**, 251 (2019).
- [25] P. Parashar, K. A. Milton, Y. Li, H. Day, X. Guo, S. A. Fulling, and I. Cavero-Peláez, Quantum electromagnetic stress tensor in an inhomogeneous medium, *Phys. Rev. D* **97**, 125009 (2018).
- [26] V. Estesó, S. Carretero-Palacios, L. G. MacDowell, J. Fiedler, D. F. Parsons, F. Spallek, H. Míguez, C. Persson, S. Y. Buhmann, I. Brevik, and M. Boström, Premelting of ice adsorbed on a rock surface, *Phys. Chem. Chem. Phys.* **22**, 11362 (2020).
- [27] J. Luengo-Márquez and L. G. MacDowell, Lifshitz theory of wetting films at three phase coexistence: The case of ice nucleation on silver iodide (agi), *J. Colloid Interface Sci.* **590**, 527 (2021).
- [28] Y. Li, K. A. Milton, I. Brevik, O. I. Malyi, P. Thiyam, C. Persson, D. F. Parsons, and M. Boström, Premelting and formation of ice due to Casimir-Lifshitz interactions: Impact of improved parameterization for materials, *Phys. Rev. B* **105**, 014203 (2022).
- [29] J. Luengo-Marquez, F. Izquierdo-Ruiz, and L. G. MacDowell, Intermolecular forces at ice and water interfaces: Premelting, surface freezing, and regelation, *J. Chem. Phys.* **157**, 044704 (2022).
- [30] I. E. Dzyaloshinskii, E. M. Lifshitz, and L. P. Pitaevskii, The general theory of van der Waals forces, *Adv. Phys.* **10**, 165 (1961).
- [31] E. Sloan, Jr. and C. Koh, *Clathrate Hydrates of Natural Gases* (CRC Press, Boca Raton, FL, 2007).
- [32] D. E. Aspnes, Local field effects and effective medium theory: A microscopic perspective, *Am. J. Phys.* **50**, 704 (1982).
- [33] O. Bonnefoy, F. Gruy, and J.-M. Herri, A priori calculation of the refractive index of some simple gas hydrates of structures I and II, *Mater. Chem. Phys.* **89**, 336 (2005).
- [34] O. Bonnefoy, F. Gruy, and J.-M. Herri, Van der Waals interactions in systems involving gas hydrates, *Fluid Phase Equilib.* **231**, 176 (2005).
- [35] D. Parsons and B. W. Ninham, Importance of accurate dynamic polarizabilities for the ionic dispersion interactions of alkali halides, *Langmuir* **26**, 1816 (2010).
- [36] J. Fiedler, P. Thiyam, A. Kurumbail, F. A. Burger, M. Walter, C. Persson, I. Brevik, D. F. Parsons, M. Boström, and S. Y. Buhmann, Effective Polarizability Models, *J. Phys. Chem. A* **121**, 9742 (2017).
- [37] *CRC Handbook of Chemistry and Physics (86th ed.)*, edited by D. R. Lide, (CRC Press, Boca Raton, FL, 2005).

- [38] O. Prieto-Ballesteros, J. S. Kargel, M. Fernandez-Sampedro, F. Selsis, E. S. Martinez, and D. L. Hogenboom, Evaluation of the possible presence of clathrate hydrates in europas icy shell or seafloor, *Icarus* **177**, 491 (2005).
- [39] E. M. Lifshitz, The theory of molecular attractive forces between solids, *Sov. Phys. JETP* **2**, 73 (1956).
- [40] Y. Li, K. A. Milton, X. Guo, G. Kennedy, and S. A. Fulling, Casimir forces in inhomogeneous media: Renormalization and the principle of virtual work, *Phys. Rev. D* **99**, 125004 (2019).
- [41] S. A. Ellingsen, Casimir attraction in multilayered plane parallel magnetodielectric systems, *J. Phys. A: Math. Theor.* **40**, 1951 (2007).
- [42] O. A. Karim and A. D. J. Haymet, The ice/water interface: A molecular dynamics simulation study, *J. Chem. Phys.* **89**, 6889 (1988).
- [43] I. Brevik, Minkowski momentum resulting from a vacuum-medium mapping procedure, and a brief review of Minkowski momentum experiments, *Ann. Phys. (NY)* **377**, 10 (2017).
- [44] T. Serwatka, R. G. Melko, A. Burkov, and P.-N. Roy, Quantum Phase Transition in the One-Dimensional Water Chain, *Phys. Rev. Lett.* **130**, 026201 (2023).
- [45] L. A. Wilen, J. S. Wettlaufer, M. Elbaum, and M. Schick, Dispersion-force effects in interfacial premelting of ice, *Phys. Rev. B* **52**, 12426 (1995).
- [46] P. Thiyam, J. Fiedler, S. Y. Buhmann, C. Persson, I. Brevik, M. Boström, and D. F. Parsons, Ice particles sink below the water surface due to a balance of salt, van der waals, and buoyancy forces, *J. Phys. Chem. C* **122**, 15311 (2018).